TESTS ON MODELS OF NUCLEAR REACTOR ELEMENTS

I.   Head Losses in Blanket Sub-Assembly

J. S. McNown
R. A. Yagle
W. W. O'Dell

ABSTRACT

For a model of a blanket sub-assembly of the proposed APDA reactor, laboratory measurements have been made of the head losses for the blanket element and for the various distributing orifices. Tests with water have been generalized so that the results provide design criteria for liquid sodium which is to be used in the reactor.

A. INTRODUCTION

Laboratory tests on the flow through the elements of a nuclear reactor are being conducted at The University of Michigan for Atomic Power Development Associates. Under an agreement between the Engineering Research Institute and APDA, Project 2431 was started on September 15, 1955. The experiments are being conducted in the fluid mechanics laboratory of the Department of Engineering Mechanics.

The studies on the blanket element include measurements and their interpretation on (1) the head loss for flow through the element, (2) the head loss through orifice plates, and (3) turbulent diffusion. Items (1) and (2) have been completed and are described in this report. Item (3) is nearly complete. Similar tests are to be conducted for a model of the fuel-element section which is being erected.

The results of the measurements of head loss in the model of the blanket element are presented in three different ways. The data obtained for tests with flowing water are presented directly. These results were then reduced to dimensionless form to show the general nature of the results and to make possible comparisons with other published information. Finally, plots were prepared for use in the design of a reactor in which liquid sodium is to be the fluid.

The project supervisor is J. S. McNown, and most of the tests and the analysis were conducted by R. A. Yagle and W. W. O'Dell. In addition, M. Cobble, G. Howell, M. Saad, L. Wolf, and M. Kaufman assisted on various phases of the project.

B. DESCRIPTION OF EXPERIMENTAL TESTS

A Plexiglas model of a blanket sub-assembly was furnished by APDA. The circulating water system of the laboratory was utilized as a source of supply. The throttling valve shown in Fig. 1 allowed for control of discharge over a wide range. The pertinent dimensions of the model are shown in Figs. 1 and 2.

Two types of head loss were measured for the blanket elements:

(a) that for established flow through the rods and
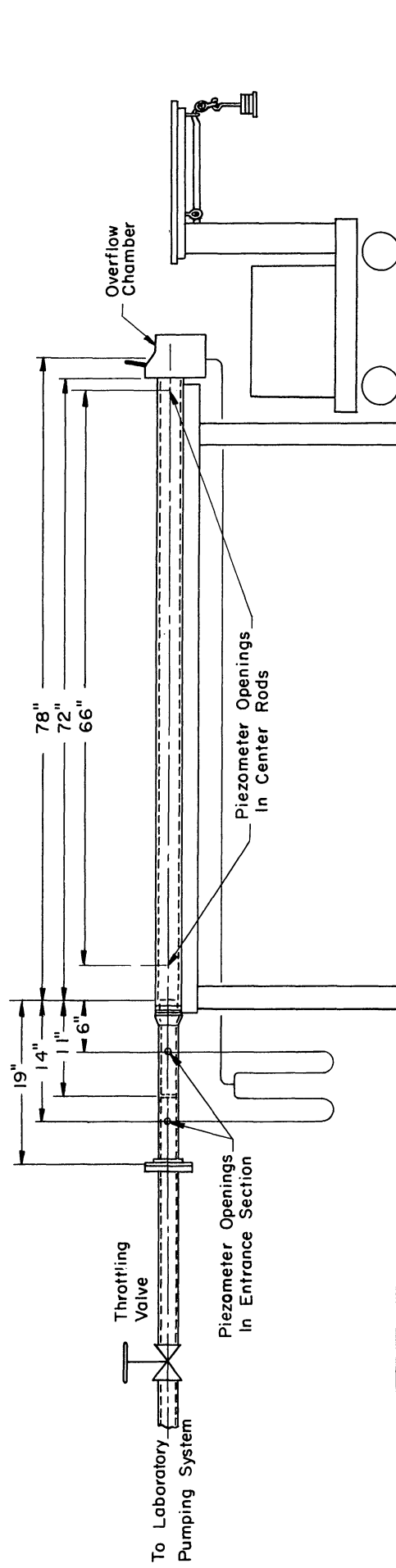(b) the overall loss between points upstream and downstream of the rod
    section.

1

Figure I

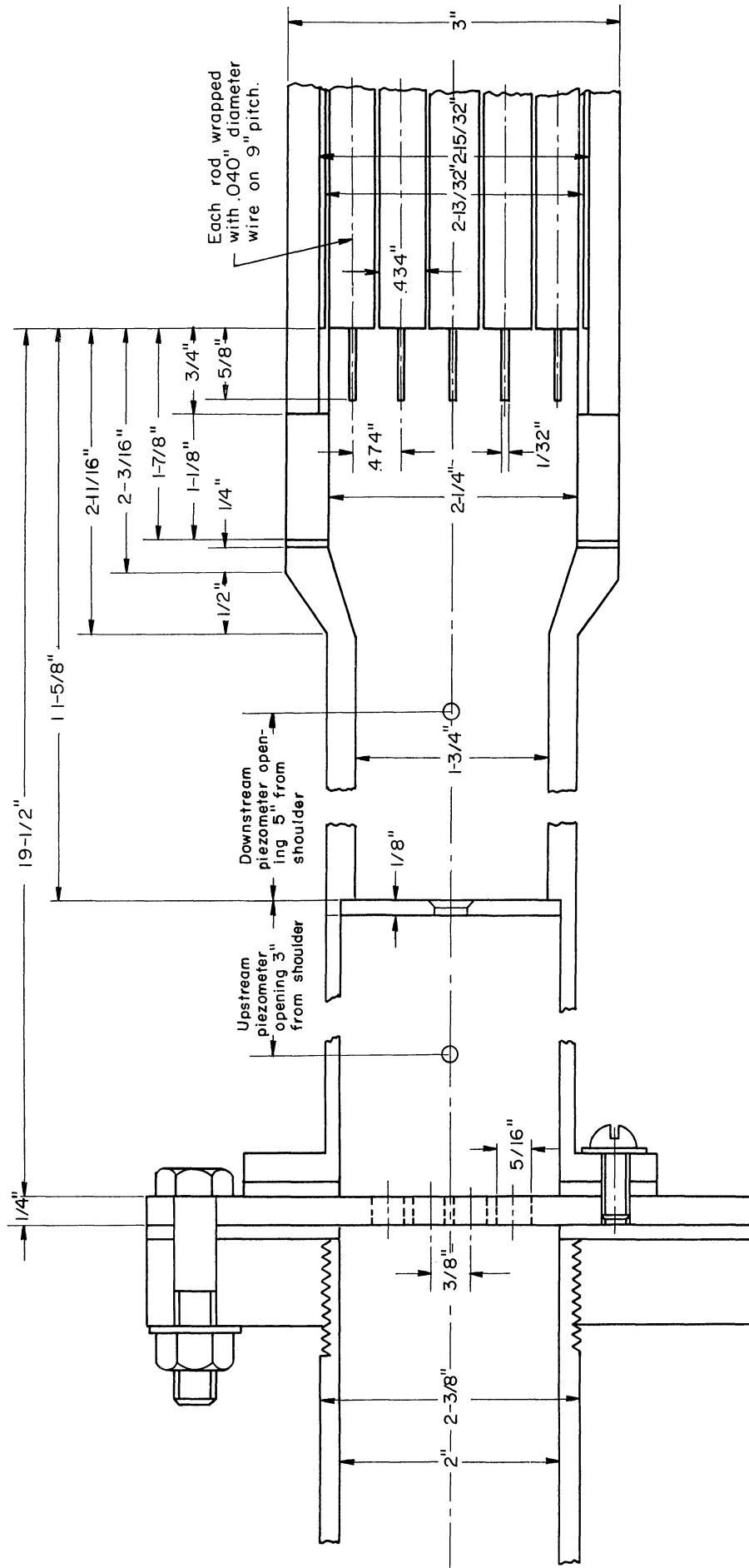General arrangement of blanket sub-assembly model.

Figure 2

Detail of orifice arrangement in entrance section.

Each rod wrapped with .040" diameter wire on 9" pitch.

3"

.434"

2-13/32" 2-15/32"

3/4"
5/8"
1/4"
1-1/8"
1-7/8"
2-3/16"
2-11/16"

.474"

2-1/4"

1/32"

1-3/4"

Downstream piezometer opening 5" from shoulder

1/8"

Upstream piezometer opening 3" from shoulder

1-5/8"

19-1/2"

1/4"

5/16"

3/8"

2-3/8"

2"

3

For the first test the center rod of the twenty-five in the sub-assembly was instrumented with rings of piezometer openings, one four inches from the upstream end, and the other two inches from the downstream end. These orifices were connected to a differential manometer and the head loss for the intervening 66 inches of the rod section was determined over the entire practicable range of flow rates. No orifices were used in these tests, the discharge being controlled by means of the throttling valve. Figure 3 is a plot of the data obtained, given as head loss in feet of water versus the discharge in cubic feet of water per second. The scatter of points at the lower flow rates is a consequence of using several different manometer systems, some of which were comparatively insensitive. The curve was drawn so that those points believed to represent the most reliable results were given the most weight. Calculated curves based on friction factors for smooth pipes and on the Hagen-Poiseuille formula are shown at the fully turbulent and fully laminar ends of the curve, respectively.

The next series of tests was made with six orifice plates placed in the entrance section of the sub-assembly As indicated in Fig 2, these orifices were placed against a shoulder eight inches from the entrance, a change from the actual design. This was done so that the effect on the flow through the orifice of the perforated plate just upsteam of the orifice would be insignificant. Two piezometer openings were made in the side of the entrance pipe three inches upstream and five inches downstream from the shoulder, and a third opening was placed in the overflow chamber at the end of the rod section. These were connected in pairs to a differential manometer. In this way the head loss across the orifice and the overall head loss in the rod section, including entrance and exit losses, were determined. Figures 4 and 5 are plots of these results over the available range of discharge. The head loss in feet of water across the orifice is given in Fig. 4, and the head loss from five inches downstream of the orifice to the overflow chamber in Fig. 5. In Fig. 5 the lower curve represents the best approximation of all the data taken, while the upper is adjusted in a manner which is explained in the next section. In Fig. 4 the solid curves for each of the orifice diameters extend only over the range of discharges actually used.

C. ANALYSIS OF EXPERIMENTAL RESULTS

Comparison of the results of the tests represented on Figs. 3, 4, and 5 with other information available requires an assessment of the importance of certain departures from standard practice. The diameter of the entrance pipe (without an insert) upstream was two inches instead of 1-3/4 inches. Also the distances of the piezometer openings upstream and downstream of the orifice plate were greater than recommended in orifice standard specifications. As a consequence, varying degrees of recovery of kinetic energy occurred for the several orifices. The distance of five inches from the orifice to the second piezometer opening was not sufficient for full recovery, especially for the smaller orifices. Thus the piezometric head at the second piezometer opening was low because of incomplete conversion of velocity head. Therefore, the overall head loss through the rod
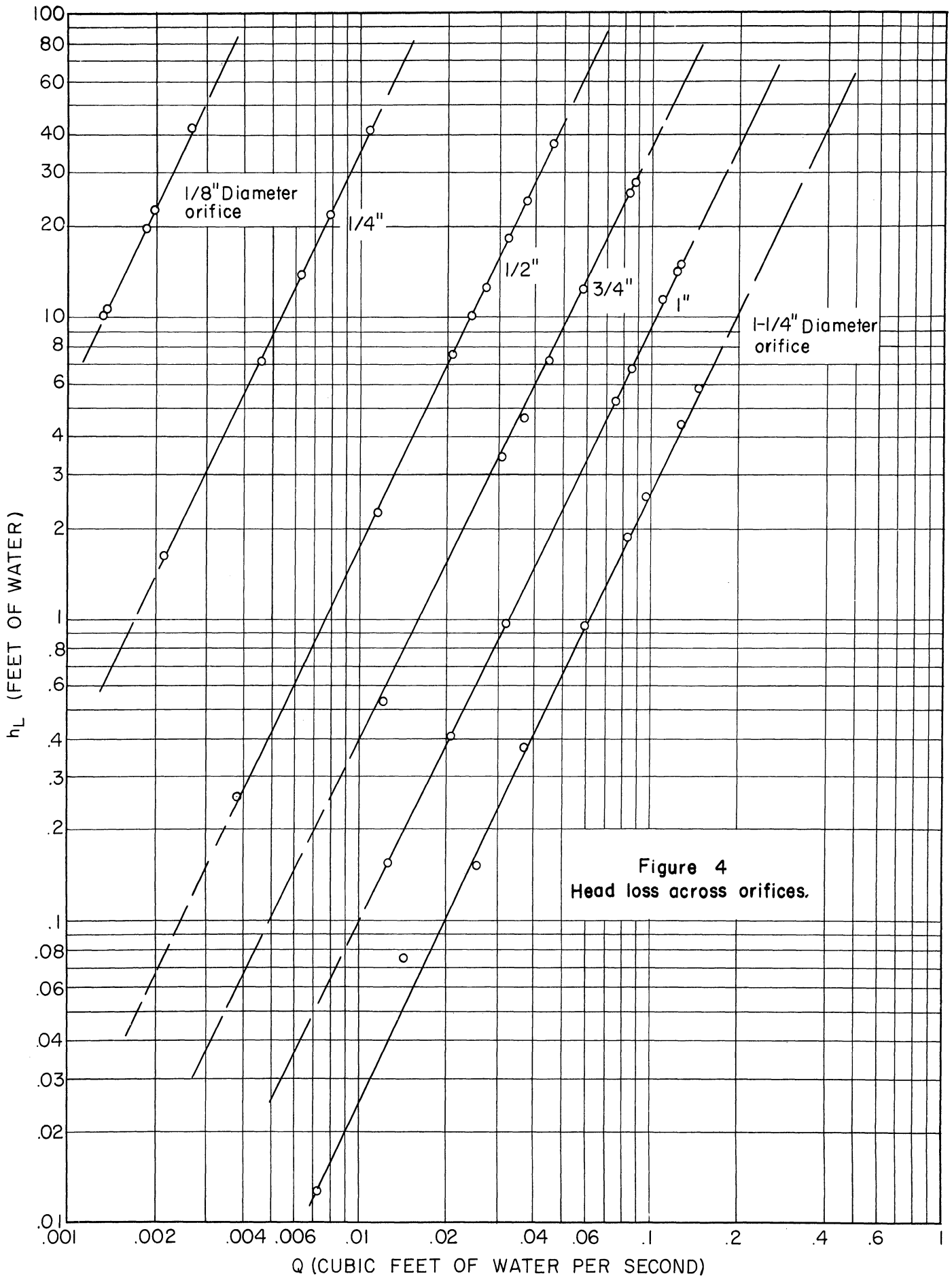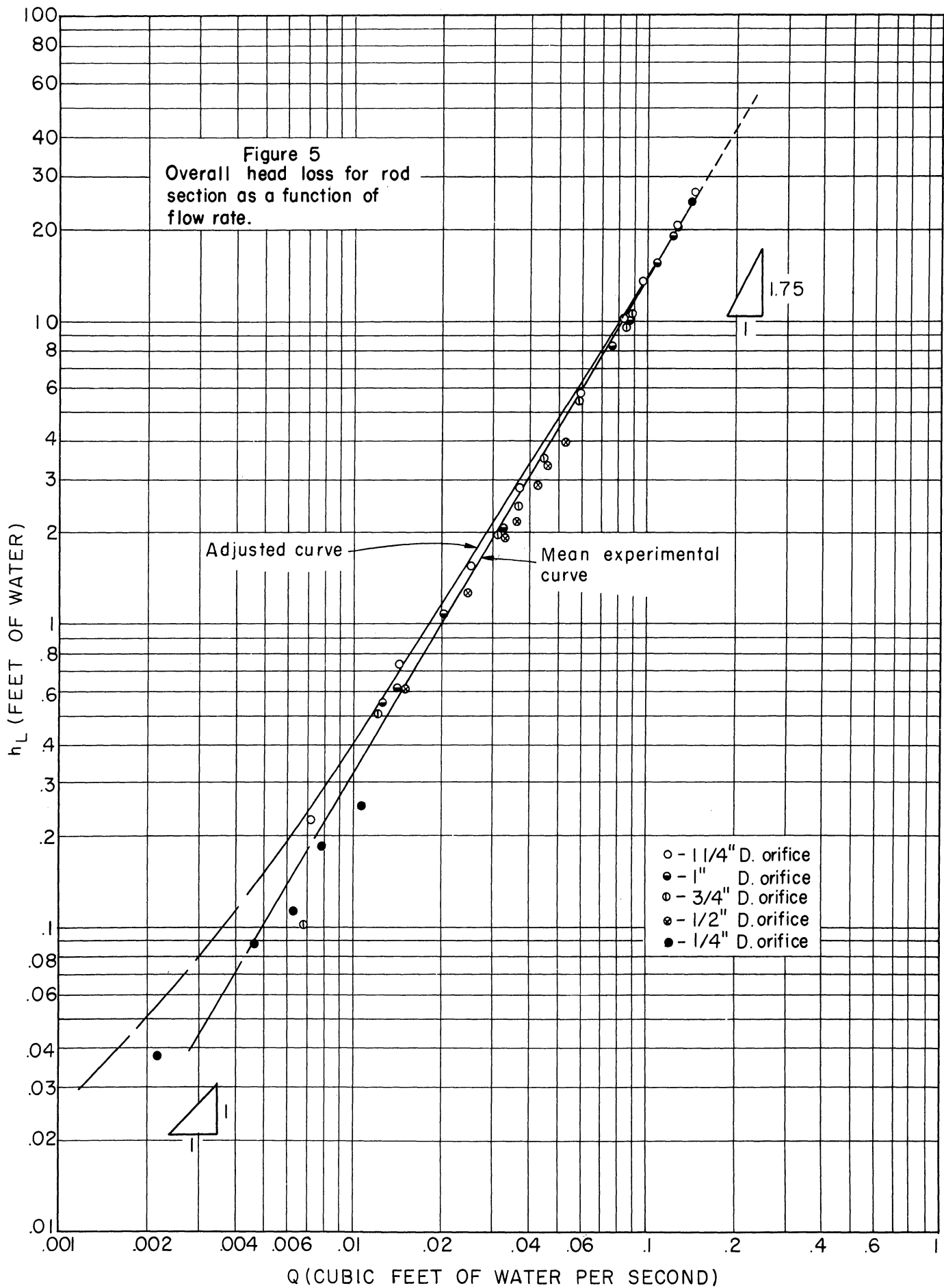
Figure 3
Head loss versus flow rate for 66 inches of rod section.
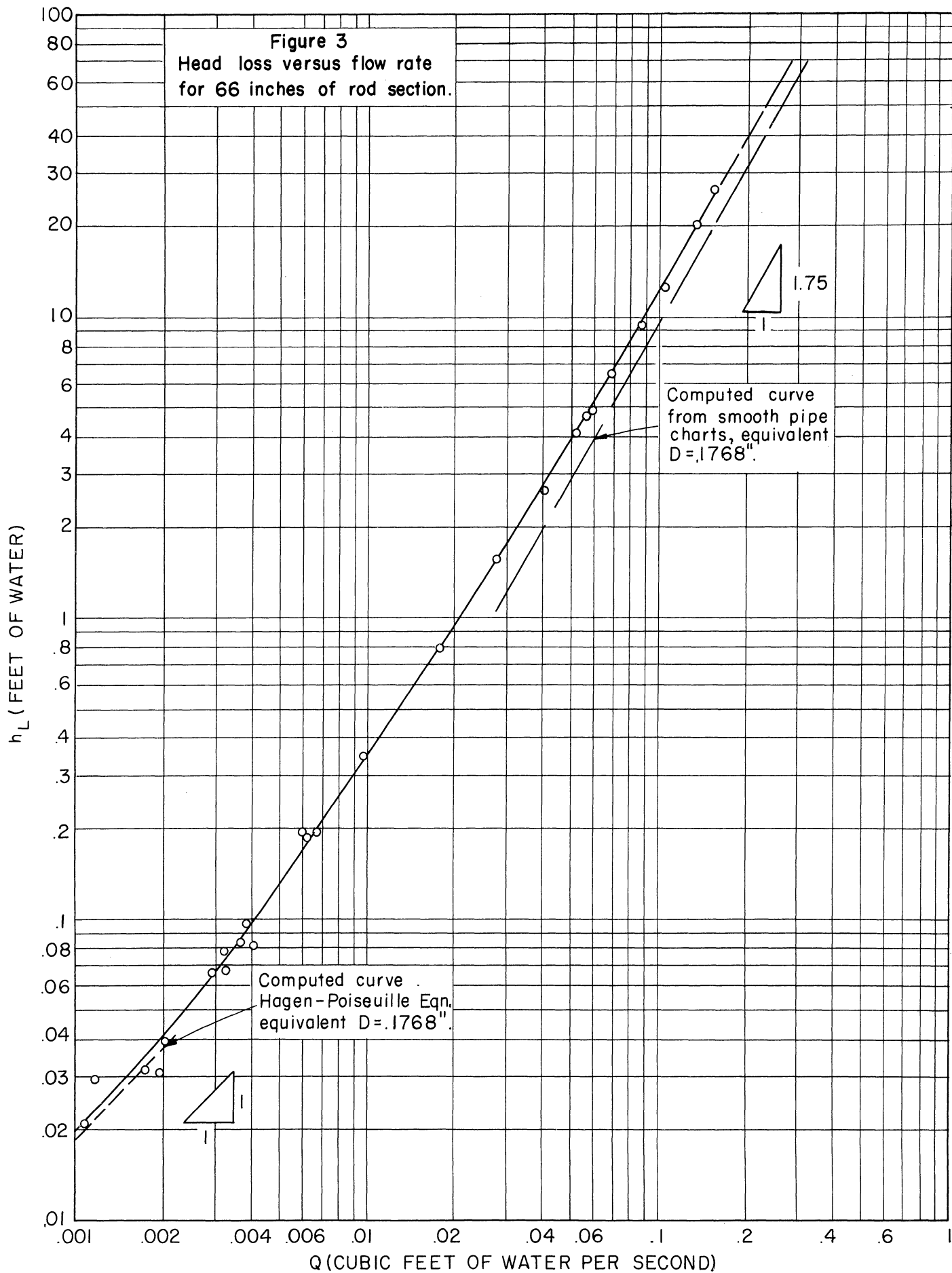
Figure 4
Head loss across orifices.

6

Figure 5
Overall head loss for rod section as a function of flow rate.

100
80
60
40
30
20

10
8
6

4
3

2

h_L (FEET OF WATER)

1
.8
.6

.4
.3

.2

.1
.08
.06

.04
.03
.02

.01

1.75
1

Adjusted curve

Mean experimental curve

1
1

o – 1 1/4" D. orifice
● – 1"   D. orifice
◑ – 3/4" D. orifice
⊗ – 1/2" D. orifice
● – 1/4" D. orifice

.001   .002   .004 .006 .01   .02   .04 .06 .1   .2   .4 .6 1

Q (CUBIC FEET OF WATER PER SECOND)

section, measured by the differential manometer, was slightly low. This can be seen by comparing head losses at the lower flow rates as given by Fig. 3 for 66 inches of the rod section with the lower curve of Fig. 5. The head loss for the entire rod section plus entrance and exit losses cannot be less than one of its component parts. Because it appeared to be less, the upper curve of Fig. 5 was adjusted in a consistent manner by assuming the recovery to be complete at the second piezometer opening.

The difference in piezometric head can be computed from Bernoulli's equation if the loss term for the expansion after the orifice is included;

$$\frac{V_1^2}{2g} + \frac{P_1}{\gamma} = \frac{V_2^2}{2g} + \frac{P_2}{\gamma} + \frac{(V_j - V_2)^2}{2g} \quad , \tag{1}$$

in which V_1 is the average velocity in the two-inch-diameter section, V_2 the average velocity in the 1-3/4-inch-diameter section, and V_j the velocity in the contracted jet coming through the orifice. The contraction coefficients used were those presented by von Mises[1] and found in many standard references.[2] The differences between the computed loss and the measured loss is greatest if V_j is relatively great, as it was for the smaller orifices. A typical calculation for a point on the upper curve of Fig. 5 is given in the Appendix of this report.

The effect of the adjustment on the data of Fig. 4 was negligible. For the smaller orifices the head loss across the orifice was sufficiently large that the correction was insignificant. For the larger orifices the correction itself was small.

To ascertain that the discharge coefficients were relatively constant for the range of Reynolds numbers used, the plot given as Fig. 6 was made. The Reynolds numbers were based on the orifice diameter, the kinematic viscosity of the water at the time of testing, and the velocity V_o obtained by dividing the discharge by the orifice area. The loss coefficient K_o is defined in the conventional manner,

$$h_L = K_o \frac{V_o^2}{2g} \quad . \tag{2}$$

This type of flow is often described in terms of a discharge equation,

$$Q = C_D A_o \sqrt{2g \, h_L} \quad , \tag{3}$$

from which K_o is seen to be equal to $1/C_D^2$. Within experimental error, the value of K_o is constant throughout the range of discharge in the experiments, and these
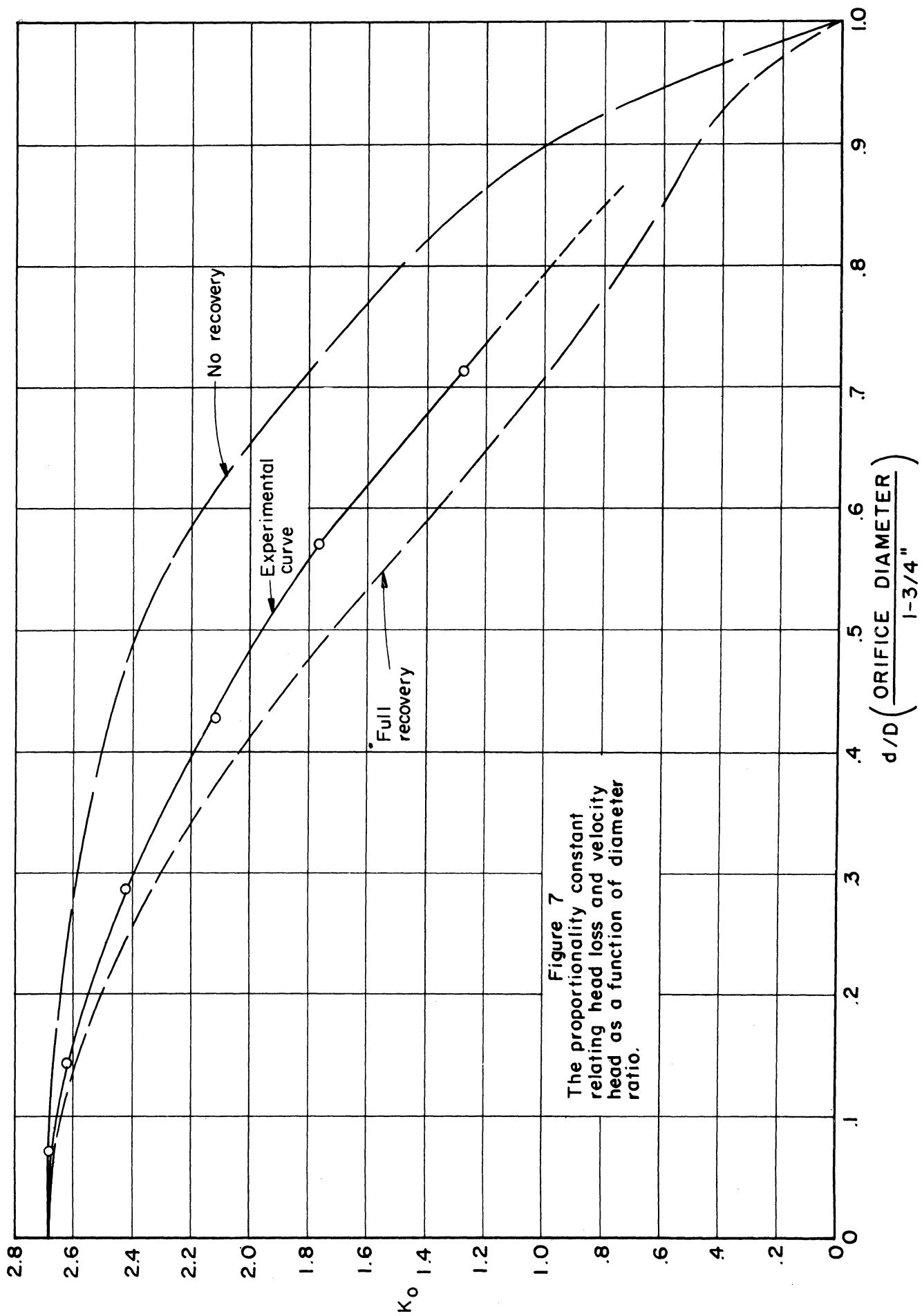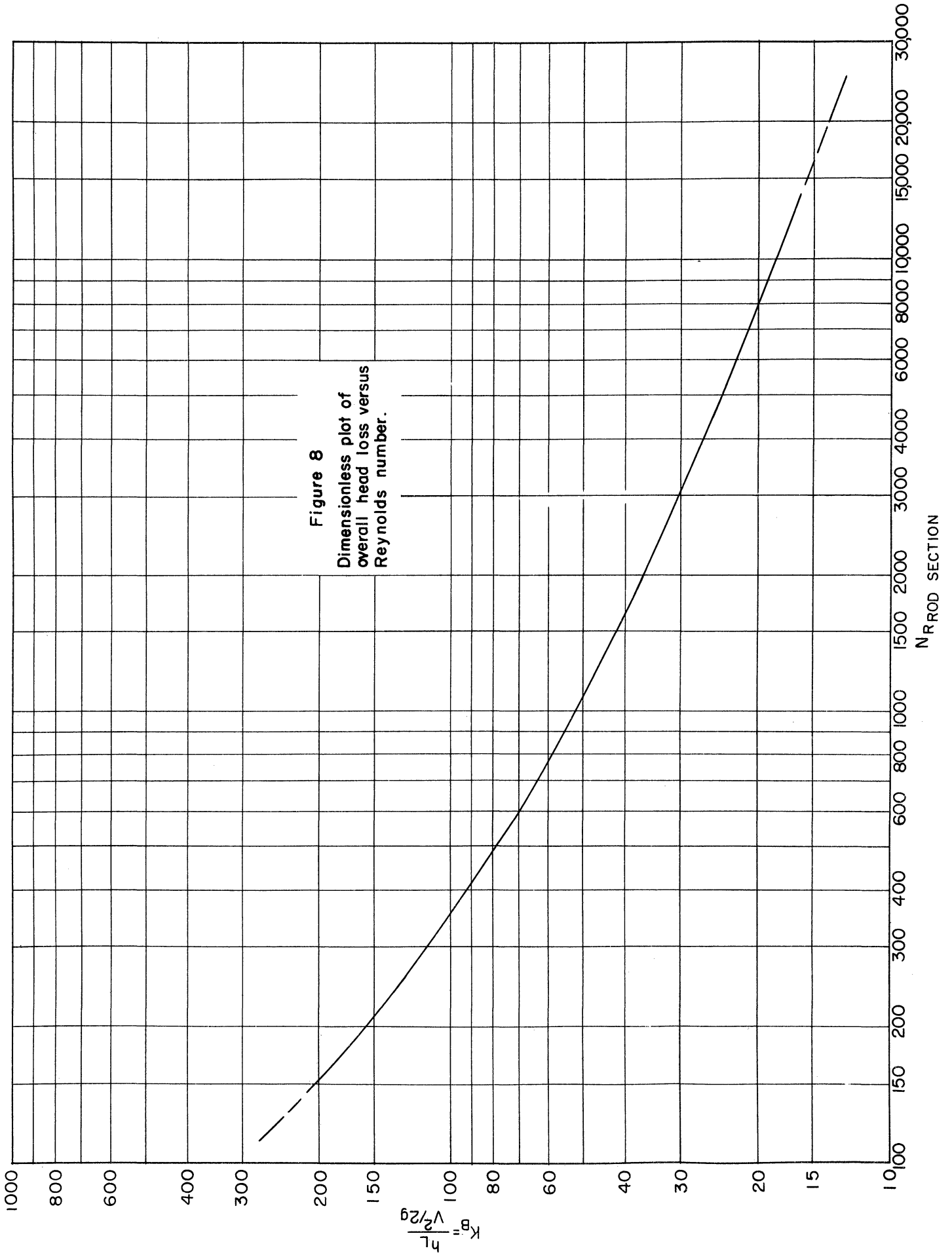
Figure 6
Loss coefficient versus Reynolds number for 6 orifice diameters
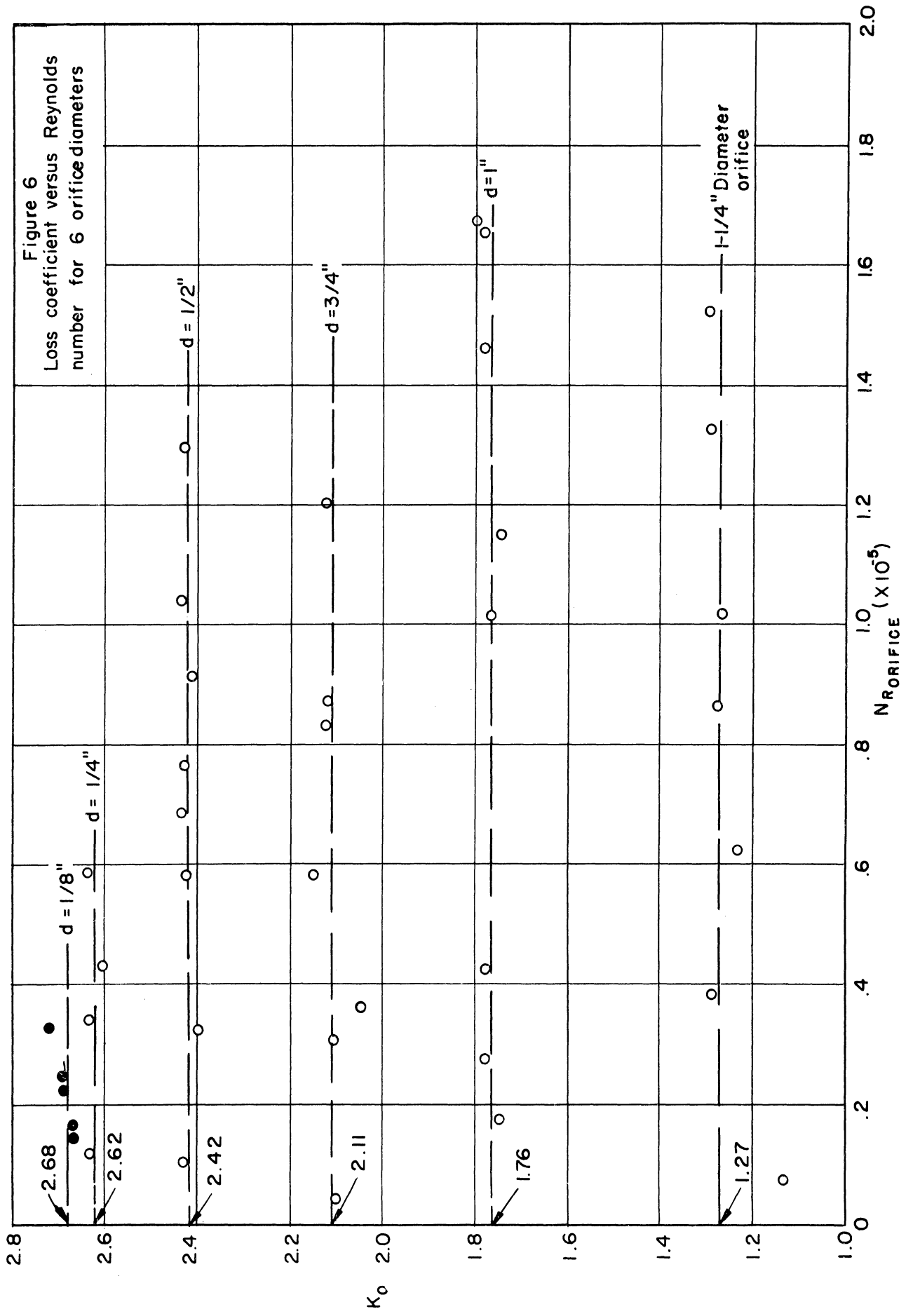
Figure 7
The proportionality constant relating head loss and velocity head as a function of diameter ratio.

10

Figure 8
Dimensionless plot of
overall head loss versus
Reynolds number.

$N_{R_{ROD\ SECTION}}$

$K_B = \dfrac{h_L}{V^2/2g}$

11

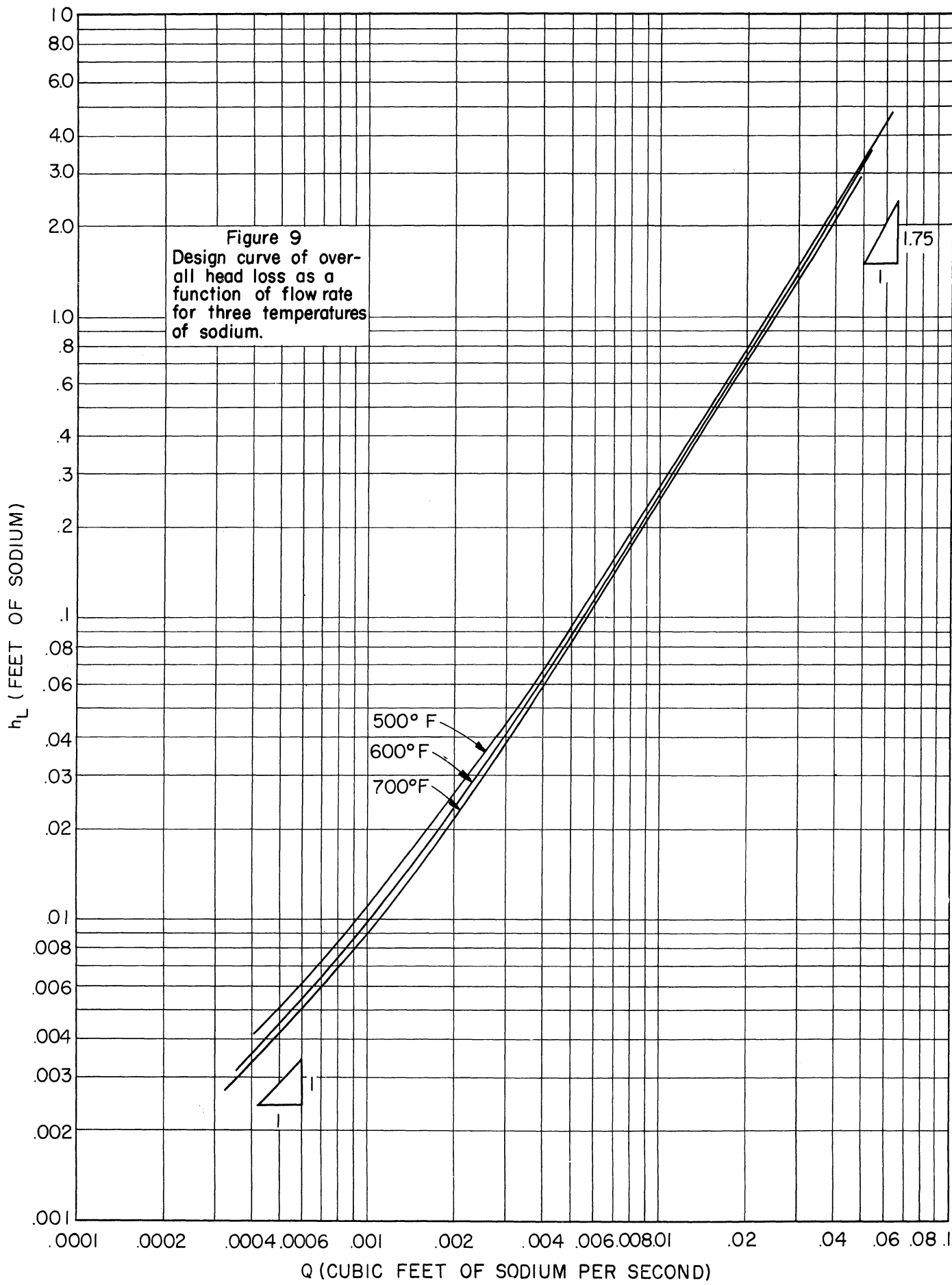constant values are representative of the respective orifices.

Slight variations from a well-machined upstream edge of the orifice opening or in the actual value of the orifice diameter can affect K_o significantly. Perhaps even more important is the short-tube effect which takes places if the orifice diameter is not much larger than the longitudinal dimension of the opening. All the orifice plates were originally made with the downstream side of the opening tapered until the length of the cylindrical portion of the orifices was 1/16 inch. For the 1/8-inch-diameter orifice this length was evidently too great and the very low value of 1.3 was obtained for K_o. A new 1/8-inch orifice was made so that the longitudinal dimension was 1/32 inch and a value of 2.68 was obtained which fits the trend shown in Fig. 6. The larger orifices were found to be free of this effect, but only because the longitudinal dimensions of the holes were less than one-quarter of the orifice diameters.
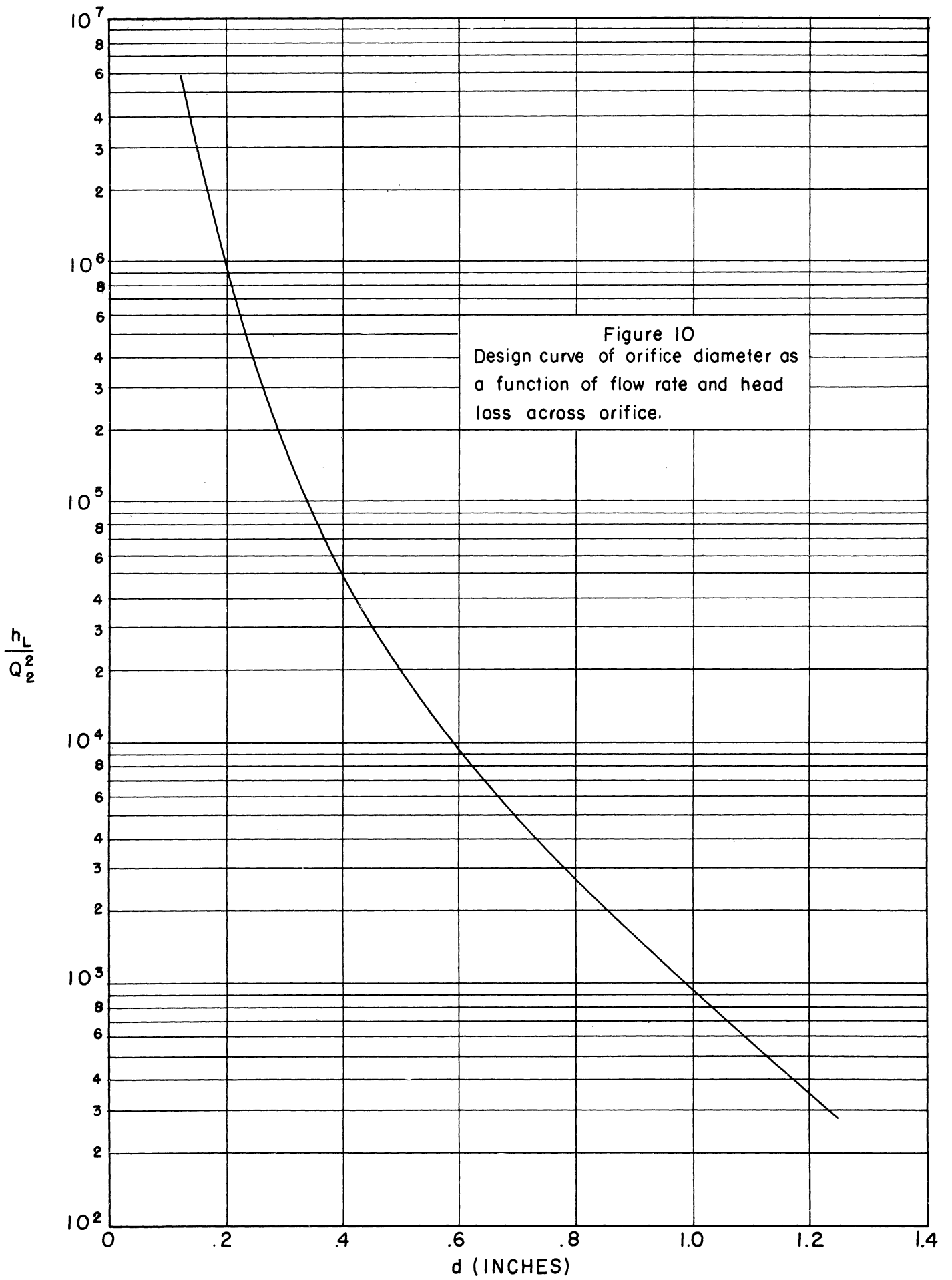
The data presented in Fig. 6 are replotted as the middle curve of K_o versus d/D in Fig. 7. Again some variation from the usual plots of such values can be noted by comparison with the other two curves plotted on the same figure. The upper curve represents K_o, or $1/C_D^2$, based on accepted data for sharp-edged orifices.[3] Because the piezometer openings were close to the orifice no recovery of kinetic energy has taken place. The lower curve was calculated for complete recovery, again using contraction coefficients after von Mises and the loss term as indicated in Equation 1. A typical calculation is presented in the Appendix. That the experimental curve falls between the two other curves is to be expected in that only partial recovery was achieved since the data presented in Fig. 4 were not adjusted. The relatively short entrance section after the orifice, even with the orifices further upstream than in the model, tends to make the experimental curve realistic as a basis for design.

Figure 8 is a dimensionless plot of the corrected data presented in Fig. 4. K_b, the overall head loss in the rod section, including entrance and exit losses, divided by the velocity head in the rod section, is plotted against the Reynolds number of the flow in the rod section. This Reynolds number is based on an equivalent diameter of .177 inch and the velocity on an open area of 2.07 square inches. The computations of this diameter and area are also shown in the Appendix. This type of plot is applicable to flow of any fluid through the model. Consequently, its use was a logical intermediate step in the preparation of the design plots presented in the next section of this report.

D. APPLICATION OF EXPERIMENTAL DATA TO DESIGN

Two plots based on the preceding analysis, Figs. 9 and 10, have been made in order to indicate how orifices may be selected to achieve a certain discharge of liquid sodium in the blanket sub-assemblies of the reactor. For a given element, data on heat transfer will govern the selection of the appropriate discharge. Also a certain head is available in the plenum chamber leading to these sub-assemblies.

Figure 9
Design curve of over-
all head loss as a
function of flow rate
for three temperatures
of sodium.

h_L (FEET OF SODIUM)

Q (CUBIC FEET OF SODIUM PER SECOND)

13

Figure 10
Design curve of orifice diameter as a function of flow rate and head loss across orifice.

$\frac{h_L}{Q_2^2}$

d (INCHES)

14

Hence, the ideal curves should (1) indicate for the selected discharge the amount of head loss to be expected in the sub-assembly exclusive of the orifice, and (2) make possible the selection of the proper orifice diameter to cause the remainder of the available head to be lost as the sodium passes through the orifice.

Figure 9 is a plot of head loss for the rod section in feet of sodium at three temperatures versus the discharge in cubic feet of sodium per second. Figure 10 is a plot of head loss across the orifice (in feet of sodium) divided by the square of the discharge versus orifice diameter in inches. Figure 9 was obtained from the dimensionless plot of Fig. 8. Simultaneous values of K_b and Reynolds number were read from Fig. 8 and reduced to the desired design form. The discharge of sodium corresponding to a Reynolds number was calculated, using the kinematic viscosity from curves supplied by APDA[4] and the equivalent diameter of the rod section. The appropriate head corresponding to this discharge was obtained by multiplying K_b by the velocity head. A typical calculation using this method is given in the Appendix. Figure 10 represents Equations 2 or 3 rearranged in the form

$$\frac{h_L}{Q^2} = \frac{1}{C_D{}^2 \, A_o{}^2 \, 2g} = \frac{16K_o}{\pi^2 d^4 2g} = \frac{522K_o}{d^4} \tag{4}$$

The various plots presented in this report represent data obtained over a wide range of conditions. If, nonetheless, values outside the range of these data are required, the results presented can be extrapolated on the basis of well-established trends for either higher or lower flow rates. The slopes at the ends of the head-loss curves are accordingly indicated on the plots.

APPENDIX

(1) Calculation of Open Area in Rod Section of Sub-Assembly:

Frontal Area   2.406 inches square or 5.80 square inches.
Solid Area   25 rods of .434-inch diameter or 3.70 square inches.
              25 wires of .040-inch diameter or .0315 square inch.
Open Area   2.07 square inches.

(2) Calculation of Equivalent Diameter of Rod Section of Sub-Assembly:

Cross-Sectional Area   2.07 square inches.
Wetted Perimeter   4 sides of 2.406 inches
                        25 rods of $\pi(.434)$ inches circumference
                        25 wires of $\pi(.040)$ inch circumference.
Hydraulic Radius   cross-sectional area of 2.07 square inches divided
                        by wetted perimeter of 46.88 inches or .0442 inch.
Equivalent Diameter   4 times the hydraulic radius or .177 inch.

(3) Calculation of Computed Curve of Fig. 3 for Hagen-Poiseuille Equation:

$$h_L = \frac{32\nu V L}{g d^2} = \frac{32(1.059 \times 10^{-5})\, V\, 66/12}{32.2\,(.177/12)^2} = .267V = \frac{.267Q(144)}{2.07} = 18.6Q$$

with kinematic viscosity ν for 70°F.

(4) Calculation of Typical Point on Computed Curve of Fig. 3, Using Smooth-Pipe
     Charts:

Assume Q of .1 cfs or V of 6.96 fps.

$$N_R = \frac{Vd}{\nu} = \frac{6.96(.177/12)}{(1.059 \times 10^{-5})} = 9700 \ .$$

Corresponding friction factor f for smooth-pipe curve is .033.

$$h_L = f\,\frac{L}{d}\,\frac{V^2}{2g} = .033\,\frac{66}{.177}\,\frac{(6.96)^2}{64.4} = 9.7 \text{ feet of water.}$$

16

(5) Calculation of a Typical Point on Adjusted Curve of Fig. 5:

    (a) For 3/4-inch-diameter orifice, d/D = .75/1.75 = .428. Corresponding von Mises C_c is .635 and V_j is 5.13 fps.

$$\frac{V_1{}^2}{2g} + \frac{P_1}{\gamma} = \frac{V_2{}^2}{2g} + \frac{P_2}{\gamma} + \frac{(V_j - V_2)^2}{2g} \qquad \text{(Equation 1)}$$

For Q of .01 cfs,

$$h_L = .00556 + .3195 - .00326 = .3218 \text{ foot of water.}$$

Figure 4 gives h_L of .40 foot of water, so a mean curve through experimental points for this orifice on Fig. 5 should be raised approximately .08, or from .32 to .40 foot of water.

    (b) For 1/4-inch-diameter orifice, d/D = .25/1.75 = .1428. Corresponding von Mises C_c is .614 and V_j is 47.8 fps. Equation 1 with values substituted for Q of .01 cfs,

$$h_L = .00556 + 34.5 - .00326 = 34.50 \text{ feet of water.}$$

Figure 4 gives h_L of 34.65 feet of water, so a mean curve through experimental points for this orifice of Fig. 5 should be rasied approximately .15, or from .25 to .40 foot of water.

(6) Calculation of a Typical Point on Lower Curve of Fig. 7.

Equation 1 with Q divided by appropriate areas substituted for various V terms can be written as

$$h_L = \frac{Q^2}{2g}\left[\frac{1}{A_2{}^2} - \frac{1}{A_1{}^2} + \left(\frac{1}{C_c A_o} - \frac{1}{A_2}\right)^2\right] .$$

From Equation 3

$$K_o = \frac{1}{C_D{}^2} = \frac{A_o{}^2 2gh_L}{Q^2} = A_o{}^2\left[\frac{1}{A_2{}^2} - \frac{1}{A_1{}^2} + \left(\frac{1}{C_c A_o} - \frac{1}{A_2}\right)^2\right] .$$

For a d/D of .5, for example, von Mises C_c is .644 and d is .875 inch. Thus A_o and $C_c A_o$ can be found. A_1 and A_2 are based on 2-inch and 1-3/4-inch diameters, respectively. K_o is therefore 1.717.

(7) Calculation of a Typical Point on 500°F Curve of Fig. 9:

       For a Reynolds number of 1863 (representing a flow rate of .02 cfs of water) the corresponding K_b, or h_L divided by $V^2/2g$, from Fig. 8 is 38.20. The Q of sodium for this Reynolds number is .00842 cfs, based on a kinematic viscosity of 4.56×10^{-6} feet squared per second for the sodium and the equivalent diameter of .177 inch and an open area of 2.07 square inches. This gives a velocity of .585 fps, and the corresponding h_L is .203 foot of sodium.

REFERENCES

(1) von Mises, R., "Berechnung von Ausfluss and Überfallzahlen," VDI Zeitschrift, 1917.

(2) Rouse, H., Elementary Mechanics of Fluids. New York: John Wiley and Sons, Inc., 1950, p. 57.

(3) Rouse, H., and Abul-Fetouh, A. H., "Characteristics of Irrotational Flow Through Axially Symmetric Orifices," Trans. ASME, 17: 421-426 (1950).

(4) Liquid Metals Handbook, 3rd ed. (Sodium, NaK, Supplement), published by the Atomic Energy Commission and the Department of the Navy, Washington, D.C., 1 July 1955, pp. 26-27.